A&A 381, L77–L80 (2002)
DOI: 10.1051/0004-6361:20011706

Astronomy & Astrophysics

Letter to the Editor

Net circular polarization of sunspot penumbrae

Symmetry breaking through anomalous dispersion

R. Schlichenmaier, D. A. N. Müller, O. Steiner, and M. Stix

Kiepenheuer-Institut für Sonnenphysik, Schöneckstr. 6, 79104 Freiburg, Germany
e-mail: schliche,dmueller,steiner,stix@kis.uni-freiburg.de

Received 23 November 2001 / Accepted 1 December 2001

Abstract. The net circular polarization, N, is used as a measure for the asymmetry of Stokes-V profiles: $N \equiv \int V(\lambda)\,\mathrm{d}\lambda$, integrated over an absorption line. Exemplary for Fe I 630.2 nm and Fe I 1564.8 nm, we synthesize penumbral V-profiles that stem from a model atmosphere in which the Evershed flow is confined to horizontal flux tubes which are embedded in a magnetic field that has the same magnetic field strength as the flow channel, but is less inclined w.r.t. the surface normal. At the two points where a line-of-sight enters and leaves the flow channel, discontinuities in the inclination, γ, the velocity v, and the azimuth, ϕ, of the magnetic field vector w.r.t. the plane perpendicular to the line-of-sight produce V-asymmetries. Assuming an axially symmetric penumbra, we investigate the azimuthal dependence $N(\psi)$ for a mid-penumbral radius. We find: (1) Without including anomalous dispersion, $N(\psi)$ is symmetric w.r.t. the line that connects disk center to the center of the spot. (2) Including anomalous dispersion, this symmetry is broken. We demonstrate that this is due to the difference in azimuth, $\triangle\phi(\psi)$, between the flow channel and the background that varies along the penumbral circle. For Fe I 630.2 nm this effect is found to be of minor relevance leading to essentially symmetric N-maps, whereas strong asymmetries are predicted for Fe I 1564.8 nm. Our results provide an explanation for recent observational findings.

Key words. sunspots – Sun: magnetic field – Sun: photosphere – techniques: polarimetric – techniques: spectroscopic

1. Introduction

In order to disentangle the physics of the fine structure in sunspot penumbrae, spectropolarimetry with high spatial and spectral resolution in absorption lines of diverse magnetic sensitivities, heights of formation, and wavelengths plays a crucial role. Two approaches are promising: (1) Inverting the measured Stokes vector to obtain a model atmosphere (e.g., del Toro Iniesta et al. 2001; Westendorp Plaza et al. 2001a,b), or (2) comparing specific properties of the measured Stokes vector with synthetic profiles that stem from model atmospheres (e.g., Maltby 1964; Landman & Finn 1979; Skumanich & Lites 1987; Solanki & Montavon 1993; Sanchez Almeida et al. 1996; Martínez Pillet 2000; Schlichenmaier & Collados 2001). In this contribution we have chosen the latter method.

The penumbral fine structure gives rise to asymmetries in spectral profiles of the Stokes parameters. In general, a velocity gradient or discontinuity along the line-of-sight (LOS) is necessary to generate Stokes asymmetries, while a gradient or discontinuity in the magnetic field can significantly alter and enhance the asymmetries (see, e.g., Auer & Heasley 1978; Sanchez Almeida & Lites 1992). Here, we restrict ourselves to asymmetry properties of Stokes-V profiles. One way to quantify the asymmetry is the net circular polarization, $N \equiv \int V(\lambda)\,\mathrm{d}\lambda$, where the integration ranges over a full absorption line.

First measurements of a non-zero net circular polarization in sunspot penumbrae have been performed by Illing et al. (1974a,b) in a broad band filter (10 nm around 530 nm). In order to compare measurements with synthetic lines, however, it is more appropriate to concentrate on the circular polarization of single absorption lines. Measurements of the net circular polarization of sunspot penumbrae in single absorption lines have been presented by Westendorp Plaza et al. (2001b) in Fe I 630.2 nm and by Schlichenmaier & Collados (2001) in Fe I 1564.8 nm. Surprisingly, sunspot maps of N in Fe I 630.2 are symmetric w.r.t. the line that connects disk with spot center, while N-maps in Fe I 1564.8 do not show that symmetry. Quite contrarily, there is a trend that the latter maps are antisymmetric. To understand this puzzling finding, we

Send offprint requests to: R. Schlichenmaier,
e-mail: schliche@kis.uni-freiburg.de

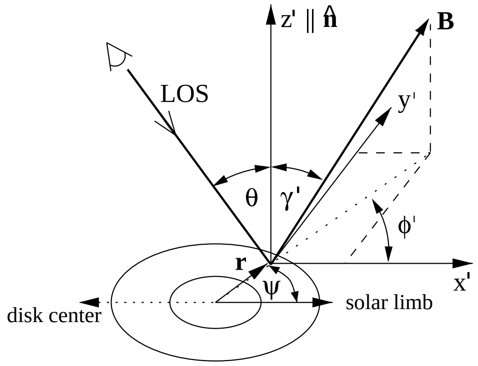

Fig. 1. A vector, $\boldsymbol{B}$, with polar coordinates (r, ψ) w.r.t. the center of the spot can be described within a local Cartesian coordinate system (x', y', z') of which the (x', y')-plane lies in the sunspot surface. The x'-axis is parallel to the line which connects disk and spot center pointing toward the solar limb. The figure sketches the inclination, γ' w.r.t. the surface normal $\hat{\boldsymbol{n}}$ (which is parallel to the z'-axis), and the azimuth, ϕ' w.r.t. the x'-axis, of $\boldsymbol{B}$. Note that the LOS is within the (x', z')-plane.

investigate the azimuthal dependence of N-maps of corresponding synthetic lines that are calculated on the basis of the moving tube model as proposed by Schlichenmaier et al. (1998, herafter SJS98). We show that the effects of anomalous dispersion[1] (see, e.g., Landolfi & Landi degl'Innocenti 1996, hereafter LL96, and references therein) play a crucial role for the creation of N.

In Sect. 2 we define the coordinate system of an axially symmetric sunspot and describe its transformation into a coordinate system that is relevant for the LOS and hence for the line-formation process. In Sect. 3 we describe the model atmosphere that is used to calculate synthetic lines. Section 4 presents our results and discusses the symmetry properties of N within the penumbra. In Sect. 5 we draw our conclusions.

2. Coordinate systems

A position in the surface plane of a sunspot can be given in polar coordinates (r, ψ), with r being the distance from spot center and with $\psi = 0°$ and $180°$ corresponding to the line which connects disk and spot center. This line is also referred to as the line-of-symmetry, since, e.g., the map of the line-of-sight velocity component of a radial outflow is symmetric w.r.t. this line. As depicted in Fig. 1, we introduce a local Cartesian coordinate system (x', y', z') at (r, ψ). The z'-axis is parallel to the surface normal $\hat{\boldsymbol{n}}$ and the x'-axis is parallel to the line-of-symmetry. A vector $\boldsymbol{B}$ is described by the inclination γ' w.r.t. $\hat{\boldsymbol{n}}$, and the azimuth, ϕ'. The coordinates of $\boldsymbol{B}$ in the local Cartesian system are $B_{x'} = B \sin\gamma' \cos\phi'$, $B_{y'} = B \sin\gamma' \sin\phi'$, and $B_{z'} = B \cos\gamma'$, with $B \equiv |\boldsymbol{B}|$.

For the calculation of the emanating Stokes vector, the relevant angles of the magnetic and flow field are the angles for the inclination, γ, and the azimuth, ϕ, w.r.t. the LOS. Hence, the local coordinate system has to be rotated around the y'-axis by the heliocentric angle, θ, which is the angle between the LOS and $\hat{\boldsymbol{n}}$ (see also Title et al. 1993). In the LOS coordinate system, the inclination, γ, and the azimuth, ϕ, of $\boldsymbol{B}$ are given by

$$\gamma = \arccos\left(\cos\gamma' \cos\theta - \sin\gamma' \cos\phi' \sin\theta\right), \tag{1}$$

$$\phi = \arctan\left(\frac{\sin\gamma' \sin\phi'}{\cos\gamma' \sin\theta + \sin\gamma' \cos\phi' \cos\theta}\right). \tag{2}$$

Note that $\phi' = 0$ implies $\phi = 0$. The LOS component of the flow velocity, v, with v_0 being the absolute velocity, is given by

$$v = v_0 \cos\gamma = v_0 \left(\cos\gamma' \cos\theta - \sin\gamma' \cos\phi' \sin\theta\right). \tag{3}$$

[1] Sometimes also referred to as the magneto-optical effects, Faraday effect or induced circular birefringence (see, e.g., Wittmann 1974).

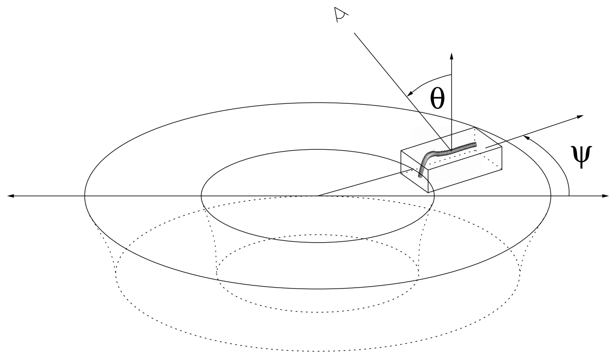

Fig. 2. Flux tube embedded in the sunspot penumbra.

3. The model

For the computation of synthetic Stokes profiles, we rely on the moving tube model of SJS98. For our calculations, we use a typical model snapshot with a flux tube breaking through the photosphere in the inner penumbra from where it bends outwards horizontally. An upflow of hot optically thick plasma enters the photosphere along the tube from below. As it flows outwards horizontally, with a flow speed of up to 14 km s^{-1}, it radiatively cools. In this paper, we concentrate on one specific radial position in the outer penumbra where the outflowing plasma has cooled off and the tube is in temperature equilibrium with the background model and has essentially the same magnetic field strength. At that location, at a radial distance of 12 000 km from spot center, the background magnetic field has an inclination of $\gamma'_{\mathrm{b}} = 65°$, while the tube is horizontal, $\gamma'_{\mathrm{t}} = 90°$. Since we assume an axially symmetric model sunspot that has no azimuthal component, the azimuth of the magnetic field, ϕ', equals the azimuthal location in the spot, ψ, i.e., $\phi' = \psi$. Along the LOS ($\theta = 15°$ in our calculations), the Unno-Rachkovsky-equations for polarized light are integrated numerically for the iron lines at 1564.8 nm and 630.2 nm (details are given in Müller 2001; Müller et al. 2001). The geometry of the tube for a certain ψ within the sunspot is sketched in Fig. 2.

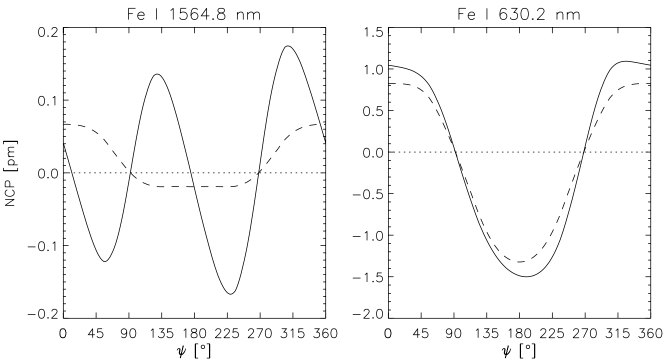

Fig. 3. *Left panel*: $N(\psi)$ for Fe I 1564.8 nm, with $\theta = 15°$. Solid line: With anomalous dispersion; dashed line: without anomalous dispersion. *Right panel*: Same as left panel, but for Fe I 630.2 nm.

The presence of a tube embedded in a penumbral background atmosphere causes discontinuities along a line-of-sight transversing it: (1) $\triangle v$, the LOS component of the flow velocity (flow channel embedded in a background at rest), (2) $\triangle\gamma$, the inclination of the magnetic field vector (horizontal flux tube in an inclined background magnetic field), and (3) $\triangle\phi$, the azimuth of the magnetic field vector w.r.t. the LOS. The discontinuity in azimuth, $\triangle\phi$, needs clarification: Although the azimuth of the tube, $\phi'_{\rm t}$ and of the background, $\phi'_{\rm b}$, are the same w.r.t. the local system, $\triangle\phi = \phi_{\rm t} - \phi_{\rm b}$ is non-zero (except for $\theta = 0°$ or $\psi = 0°$, $180°$) as a consequence of $\gamma'_{\rm t} \neq \gamma'_{\rm b}$ (cf. Eq. (2)).

Our model shares common features with the models of Solanki & Montavon (1993), Sanchez Almeida et al. (1996), and Martínez Pillet (2000), but in our case, the background is at rest and the field strength of the tube is the same as in the background model. Moreover, we concentrate on the dependence of N along an azimuthal section, i.e., along the circumference of a spot-centered circle within the penumbra at a given heliocentric angle, while the mentioned works have focussed on the center-to-limb variation of N.

4. Net circular polarization, $N(\psi)$, along an azimuthal section

With the model described in the preceding section, we calculate synthetic V-profiles along an azimuthal section for the specified radial position (12 000 km). Figure 3 displays the results for Fe I 1564.8 nm (left panel) and for Fe I 630.2 nm (right panel). The calculations are performed with (solid line) and without (dashed line) the effects of anomalous dispersion for $\theta = 15°$. For both lines, $N(\psi)$ is symmetric w.r.t. the x-axis ($\psi = 0°$ and $180°$) if the effects of anomalous dispersion are not taken into account. Including anomalous dispersion, this symmetry is broken. For Fe I 630.2 the antisymmetric component is small relative to the symmetric component. However, for Fe I 1564.8 the antisymmetric component dominates $N(\psi)$.

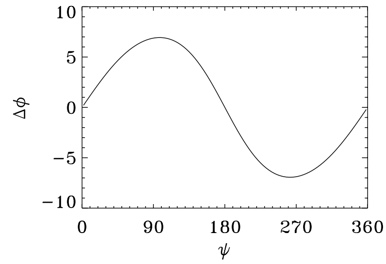

Fig. 4. The azimuthal dependence of the difference in azimuth $\triangle\phi(\psi) = \phi_{\rm t} - \phi_{\rm b}$ between the flow channel and the background magnetic field w.r.t. the LOS is displayed for a heliocentric angle of 15°. The background inclination is 65° while the flow channel is horizontal.

4.1. Symmetry properties of $N(\psi)$

To understand the antisymmetric component in $N(\psi)$, we consider the symmetry properties of the discontinuities $\triangle v(\psi)$, $\triangle\gamma(\psi)$, and $\triangle\phi(\psi)$ at the interface between the flux tube and the background, which cause the asymmetry in $V(\lambda)$. In our model, $\triangle B$ is negligible at the interface and B only slightly decreases with height. Its influence can therefore be neglected in the following discussion, but we note that $\triangle B(\psi)$ is symmetric and would not alter the following argument.

Properties of $\triangle\phi(\psi)$, $\triangle\gamma(\psi)$, and $\triangle v(\psi)$: Taking into account that $\psi = \phi'$ for an axially symmetric sunspot with no azimuthal components, it is seen from Eqs. (1)–(3) that $\gamma(\psi)$ and $v(\psi)$ are symmetric while $\phi(\psi)$ is antisymmetric w.r.t. the transformation $\psi \to -\psi$. As a consequence, $\triangle\phi(\psi) = \phi_{\rm t}(\psi) - \phi_{\rm b}(\psi)$ is antisymmetric, while $\triangle\gamma(\psi)$ and $\triangle v(\psi)$ are symmetric. In Fig. 4, $\triangle\phi(\psi)$ is plotted for a horizontal tube ($\gamma'_{\rm t} = 90°$), a background magnetic field with an inclination of $\gamma'_{\rm b} = 65°$, and a heliocentric angle of $\theta = 15°$.

$\triangle\phi$ is capable of breaking the symmetry: It has been demonstrated analytically by LL96 that along the LOS a discontinuity in the azimuth of the magnetic field vector is capable to produce a non-vanishing net circular polarization, N. Their formulas reflect that a discontinuity in ϕ along the LOS can produce a non-zero N, if and only if anomalous dispersion is included in the transfer equation of polarized light. Moreover, they demonstrate that the effect of $\triangle\phi$ on N is proportional to $\sin(2\triangle\phi)$, implying that $N = N(\triangle\phi)$ is an antisymmetric function.

Since $\triangle\gamma(\psi)$ and $\triangle v(\psi)$ are both symmetric, $N = N(\triangle\gamma(\psi), \triangle v(\psi))$ must also be symmetric w.r.t. ψ. Hence, only $\triangle\phi$ is capable to introduce an antisymmetric component in $N(\psi)$, i.e., $N(\psi)$ is composed of a symmetric contribution from $\triangle\gamma(\psi)$ and $\triangle v(\psi)$ (and from $\triangle B(\psi)$, if present) and of an antisymmetric contribution from $\triangle\phi(\psi)$. The latter contributes to N only if anomalous dispersion is included.

It can be seen in Fig. 3 that the values for N with and without anomalous dispersion are not identical where

$\triangle\phi = 0$, i.e., for $\psi = 0°, 180°$. This means that N, which is solely produced by $\triangle\gamma$ at these locations, depends on whether anomalous dispersion is included or not. In other words, switching on the anomalous dispersion introduces both, a symmetric contribution to $N(\psi)$ and the antisymmetric contribution that is caused by $\triangle\phi$.

4.2. Difference between Fe I 1564.8 nm and Fe I 630.2 nm

Having shown that $\triangle\phi(\psi)$ causes the antisymmetric component in $N(\psi)$, the question remains, why this effect is small for Fe I 630.2 nm and rather large for Fe I 1564.8 nm. Again, the work of LL96 is of help. They have found an analytical solution for a model with a single discontinuity along the LOS. In their Eqs. (18) and (19), they isolate the effects of $\triangle\gamma$ and $\triangle\phi$ on N (respectively, $\triangle\theta$, $\triangle\varphi$, v in their article). From these equations it is apparent that the weights of the symmetric contribution from $\triangle\gamma$ and the antisymmetric contribution from $\triangle\phi$ depend on the ratio between the wavelength shift due to the Doppler effect and the magnitude of the Zeeman splitting. Hence, the large difference in wavelength between Fe I 630.2 and Fe I 1564.8 is responsible for the significant difference between the two lines, since the Doppler effect depends linearly on wavelength while the Zeeman splitting is proportional to λ^2. Inserting numbers that correspond to our model into the solution of LL96, Müller (2001) estimates that the $\triangle\phi$-effect should dominate N for Fe I 1564.8 and that the $\triangle\gamma$-effect is more important for Fe I 630.2. Hence, although we cannot separate the effects of $\triangle\gamma$ and $\triangle\phi$ on N in our numerical model, the results presented in Fig. 3 can be understood on the basis of the analytical work of LL96.

4.3. Comparison with observation

Maps of the net circular polarization of sunspot penumbrae have been published by Westendorp Plaza et al. (2001b) in Fe I 630.2 nm and by Schlichenmaier & Collados (2001)[2] in Fe I 1564.8 nm. These measurements reveal that in penumbrae, $N(\psi)$ is essentially symmetric for Fe I 630.2 nm and antisymmetric for Fe I 1564.8 nm. Our theoretical results, based on synthetic lines that emanate from the moving tube model, are in full agreement with these measurements.

5. Conclusion

We demonstrate that a discontinuity in the azimuth, $\triangle\phi$, of the magnetic field vector along the line-of-sight together with the effects of anomalous dispersion plays a crucial role for the interpretation of spectropolarimetric measurements in sunspot penumbrae.

In an axially symmetric sunspot in which the magnetic and velocity field vectors have no azimuthal components, a nearly horizontal flow channel embedded in an inclined magnetic background field introduces a discontinuity, $\triangle\phi$, in the azimuth relative to the line-of-sight. Along an azimuthal section within the penumbra, $\triangle\phi(\psi)$ is antisymmetric w.r.t. the line-of-symmetry, giving rise to an antisymmetric contribution to the net circular polarization, $N(\psi)$. $N(\psi)$ consists of a symmetric contribution from $\triangle\gamma$ (and $\triangle B$ which, however, is negligible in our model configuration) and an antisymmetric contribution from $\triangle\phi$. The wavelength shift ratio between the Doppler and the Zeeman effect determines the relative weights of these two contributions to N. The difference between the symmetry properties of N-maps in Fe I 1564.8 nm and Fe I 630.2 nm can therefore be attributed to the large wavelength difference between the two lines.

The striking difference between observed N-maps for the Fe I 1564.8 and the Fe I 630.2 line can be reproduced by synthetic lines that emanate from a model atmosphere which is based on the moving tube model of SJS98. In this respect, the present work provides strong evidence that magnetic fields with (at least) two different inclinations with different flow velocities are present in the penumbra. It also demonstrates that the spatial distribution of $N(r, \psi)$ within the penumbra is a valuable diagnostic tool in order to test penumbral models.

[2] Note that in their Fig. 8, the umbral V-profiles are not fully contained on the chip, due to the large Zeeman-splitting. Hence the umbral values in the figure are in error.

References

Auer, L. H., & Heasley, J. N. 1978, A&A, 64, 67
del Toro Iniesta, J. C., Bellot Rubio, L. R., & Collados, M. 2001, ApJ, 549, L139
Illing, R. M. E., Landman, D. A., & Mickey, D. L. 1974a, A&A, 35, 327
Illing, R. M. E., Landman, D. A., & Mickey, D. L. 1974b, A&A, 37, 97
Landman, D. A., & Finn, G. D. 1979, Sol. Phys., 63, 221
Landolfi, M., & Landi degl'Innocenti, E. 1996, Sol. Phys., 164, 191
Maltby, P. 1964, Astrophysica Norvegica, 8, 205
Martínez Pillet, V. 2000, A&A, 361, 734
Müller, D. A. N. 2001, Diploma Thesis, University of Freiburg
Müller, D. A. N., Schlichenmaier, R., Steiner, O., & Stix, M. 2001, in preparation
Sanchez Almeida, J., Landi Degl'Innocenti, E., Martínez Pillet, V., & Lites, B. W. 1996, ApJ, 466, 537
Sanchez Almeida, J., & Lites, B. W. 1992, ApJ, 398, 359
Schlichenmaier, R., & Collados, M. 2001, A&A, in press
Schlichenmaier, R., Jahn, K., & Schmidt, H. U. 1998, A&A, 337, 897
Skumanich, A., & Lites, B. W. 1987, ApJ, 322, 483
Solanki, S. K., & Montavon, C. A. P. 1993, A&A, 275, 283
Title, A. M., Frank, Z. A., Shine, R. A., et al. 1993, ApJ, 403, 780
Westendorp Plaza, C., del Toro Iniesta, J. C., Ruiz Cobo, B., & Martínez Pillet, V. 2001a, ApJ, 547, 1148
Westendorp Plaza, C., del Toro Iniesta, J. C., Ruiz Cobo, B., et al. 2001b, ApJ, 547, 1130
Wittmann, A. 1974, Sol. Phys., 35, 11